Available online at www.sciencedirect.com
ScienceDirect
Ceramics International 35 (2009) 1385–1389
CERAMICS INTERNATIONAL
www.elsevier.com/locate/ceramint

The effect of lithium oxide on the threshold field of ZnO varistors

Mourad Houabes [a,*], Renaud Metz [b,c]

[a] Department Electrotechnique Université Annaba BP12 Annaba, Algérie
[b] Laboratoire Hydrazines et Procédés, UMR 5179 Lyon1-CNRS-ISOCHEM (Groupe SNPE), Université Claude Bernard Lyon1, 22 Avenue Gaston Berger, bâtiment Berthollet 69622 Villeurbanne Cedex, France
[c] Institut Charles Gerhardt, UMR 5253 Université Montpellier 2, Composante physicochimie des Matériaux Organisés Fonctionnels, CC 1700, Place Eugène Bataillon, 34095 Montpellier Cedex 5, France

Received 20 November 2006; received in revised form 16 July 2007; accepted 14 July 2008
Available online 5 August 2008

Abstract

Lithium oxide in form of Li_2CO_3 solution is added with contents of 0–200 ppm to two ZnO-based varistors standard formulations, once with Sb_2O_3 and the other without. According to Li_2CO_3 concentration, both threshold field and energy absorption capability evolution are studied. It is found that with the benefit of antimony, the lithium allows reaching high threshold field but concomitantly, low energy absorption capability. Without antimony, threshold fields up to 300 V/mm are attained, associated with a fair energy absorption capability. With 100 ppm of Li_2CO_3, optimum couple of values (315 V/mm; 115 J/cm^3) is achieved. With 200 ppm of Li_2CO_3, threshold field exceeds 500 V/mm but energy absorption capability falls below 50 J/cm^3. Correlations with SEM microstructures observations suggest that lithium increases voltage barrier height by decreasing donor density and that spinel phases ($Zn_7Sb_2O_{12}$) have detrimental effects on the electrical absorption capability by limiting the density of current, reducing the effective current path from one ZnO grain to another.
© 2008 Elsevier Ltd and Techna Group S.r.l. All rights reserved.

Keywords: C. Electrical properties; E. Varistors; ZnO-based ceramics

1. Introduction

ZnO-based varistor ceramics are non-ohmic semi-conductor component, which has ZnO as the principal ingredient and other oxide additives such as Sb_2O_3, Bi_2O_3, CoO, Mn_2O_3 and Cr_2O_3. Their high non linearity as well as good energy absorption capability of current pulses make them widely applied in electric systems as surge arresters. The market of the formers requests highest threshold field and simultaneously, ability to absorb energy upper than 100 J/cm^3 [1–3].

The non linearity coefficient α, threshold field E_s and leakage current I_f are significant parameters which characterize ZnO-based ceramics. Values of α ranging between 30 and 50 and I_f below 1 mA obtained for casual ZnO varistors are satisfying [4]. However, the trend to the miniaturization of the components requests E_s values always higher.

The electrical properties of ZnO-based varistors depend on their microstructure. During the sintering process, various metal oxide additives used in the composition get distributed in such a way that the final ZnO grain size after sintering is of the order of 10 μm surrounded by oxide phases (mainly $Zn_2Bi_3Sb_3O_{14}$ pyrochlore and $Zn_7Sb_2O_{12}$ spinel phase), grain boundaries and few pores. Varistor microstructure consists of ZnO grains separated by grain boundaries providing p–n junction semi-conductor characteristic [5] where the non linear electrical behavior occurs. Finally, the varistor is defined as a multi-junction device composed of series and parallels connections of grain boundaries [6] and the threshold field is simply calculated as:

$$E_s = n\, v_b \quad (1)$$

where E_s stands for the threshold field, n the number of potential barriers per unit length along the direction of current conduction (which is generally assumed as the number of grain boundaries) and v_b the voltage drop at each barrier.

For increasing E_s two strategies are available: v_b or n increase. However, several experimental works show that v_b does not much vary from one barrier to another and is close to about 3 ± 1 V [2–5]. Thus, the second scheme seems more

* Corresponding author.
E-mail address: houabes@yahoo.fr (M. Houabes).

0272-8842/$34.00 © 2008 Elsevier Ltd and Techna Group S.r.l. All rights reserved.
doi:10.1016/j.ceramint.2008.07.009

promising. To increase barriers per unit of thickness, a reduction of the size of ZnO grains is requested. This is currently achieved by antimony addition in the ceramic formulations of about 1 mol% combine with a sintering temperature in the scope of 1200–1350 °C [1,6–7]. However, the sintering temperature can be lower (1100–1200 °C) if antimony oxide surplus 2–4mol% are implemented [4,8]. Several works aimed at this target [7–13]. Antimony acts as inhibitor against ZnO grain growth, and it is also known that sintering temperature reduction is accompanied by grain size reduction [1,10,13]. However, energy absorption capability often, if not always, decreases when ceramics are made to have higher threshold field.

The lithium influence on the varistor electric properties was already published by some authors [14]. According to them, a small lithium quantity (ppm order) added to the conventional composition boots the threshold field with a factor of 10 to 20. This fact was explained by a size effect (r_{Li^+} (0.06 nm) « $r_{Zn^{2+}}$ (0.074 nm) suggesting ease of diffusion of lithium cations into ZnO crystal lattice which has been recently experimentally confirmed [15]. But the lithium effect, on the energy absorption capability, is still not explained.

The aim of this work is to investigate the lithium influence on the varistors threshold field while simultaneously examining their energy absorption capability.

2. Experimental procedure

2.1. Samples preparation

The samples were prepared by solid-state reaction process. Various quantities of lithium in Li_2CO_3 solution, are added to the ceramic standard composition. Table 1 shows the chemical compositions used. The oxide powders are weighed and mixed by ball milling during 24 h with Li_2CO_3 solution and organic binder substances in earthenware jar with rollers and distilled water. The aqueous slurry obtained is dried at 200 °C during 10 h to produce granulates and a new dry milling of the powders is carried out during 10 h. After sieving appropriate fractions (150 μm) to extract dust and large agglomerated particles, the material is transferred to hydraulic pressing machines. Samples are in 30 mm diameter and 2 mm thickness disc form. Then, they are sintered at 1100 °C. The sintered pellets were polished and ohmic Pt–Ag contacts were realized. An annealing until 650 °C during half an hour ensures both a good mechanical and electronic bonding between the electrodes and the ceramic. Eventally the specimens are coated on the side part by an epoxy resin.

2.2. Electric tests

I–V characteristics are measured, at low currents until 10 mA, under continuous voltage. A supply (Fug HCN 0–12.5 kV, 25 mA) outputs on the sample. The current through the ceramic is measured with an amperemeter (Keithley 619). The voltage, between ceramic electrodes, is measured with a voltmeter (Racal Dana 6000) through a probe which divides the signal per 1000.

At the high current values, two shock wave generators are used, one of long duration (2 ms/0–500 A) and the other of short duration (4/10 μs–0/65 kA). The voltage and the current are visualized and measured on the screen of a numerical storage oscilloscope (Tektronix 7633).

2.3. Analyses of microstructure

Morphological analyses in the secondary electron mode on fracture surfaces, compositional analysis in backscattered electron mode and microanalysis on polished surfaces were performed using JSM-6400 scanning electron microscope (SEM). Crystallographic analysis was carried out by the use of X-ray diffraction method on sample polished surfaces. Grain sizes for the normal grains were measured using the linear intercept method, measuring between 20 and 30 grains. A stereological correction factor of 1.56 was used to convert from average intercept distance to grain diameter.

2.4. Analyses of current–voltage characteristics

From the current–voltage characteristic, the threshold field E_s (V/mm) is given at a current of 1 mA. The energy absorption capability is calculated with the approximation:

$$A = 20.8\, V_m I_m 10^{-6}\ (\mathrm{J}) \tag{2}$$

where V_m and I_m are respectively the voltage and current maxima visualized by the oscilloscope for a short duration shock of about 4/10 μs with amplitudes of 0–65 kA.

3. Results and discussions

3.1. Composition which contains Sb_2O_3

The results of Table 2 show that the threshold field E_s increases with the lithium quantities, while the energy absorption capability (A) decreases. With 200 ppm of Li_2CO_3, samples have not sustained the energy since they have exploded.

Table 1
Chemical compositions: formulation which contains Sb_2O_3 (CW) and not (CO).

Oxide (mol%)										Salts (ppm)
ZnO	Bi_2O_3	Sb_2O_3	MnO_2	Co_3O_4	Cr_2O_3	NiO	B_2O_3	MgO	Al_2O_3	Li_2CO_3
CW	95.7	1.0	1.0	0.5	0.5	0.5	0.1	0.1	0.1	0, 20, 50, 100, 200
CO	96.7	1.0	0.5	0.5	0.5	0.5	0.1	0.1	0.1	0, 20, 50, 100, 200

Table 2
Electric field: E_s and energy absorption capability: (A) of the ZnO varistors for both chemical compositions, with (CW) and without (CO) antimony, for various quantities of lithium (sintering temperature 1100 °C)

Oxide (mol%)	Li_2CO_3 salt content					Li_2CO_3 salt content					
Li_2CO_3	CW	0	20	50	100	CO	0	20	50	100	200
E_s (V/mm)		250	301	422	720		160	257	295	315	660
A (J cm^{-3})		102	82	62	16		102	92	93	115	35

The grains morphology of these compositions is presented in Fig. 1. It is observed that as Li_2CO_3 concentration rises, the number of crystals located in the grain boundaries and with a spinel structure increases leading to a size reduction of ZnO grains from 12 to 5 μm. This behavior has already been observed [16,17]. Lithium appears to favor the formation of antimony spinel phase: $Zn_7Sb_2O_{12}$. The breakdown field (E_s) increases with the lithium doping which is in agreement with formula (1).

From the accumulated knowledge of microstructure, chemistry and physic, it is now admitted that as a result of sintering, dopants are distributed in such a way in the microstructure that the surface of the ZnO grains becomes highly resistive although the grain core maintains ZnO conductivity of about 1–10 Ω cm [14]. A potential barrier results at the grain boundary. Its maximum height, i.e. for $V = 0$, can be evaluated by the following formula: [18]

$$\phi = \frac{Q_i^2}{(8\, e\, \varepsilon_0\, \varepsilon_r\, N_d)} \tag{3}$$

where Q_i is the excess charge of majority carriers trapped at the grain boundaries (in e cm^{-3}), e: electron charge ($e = |e|$), ε_0: air dielectric permittivity, ε_r: doped-ZnO relative dielectric per-

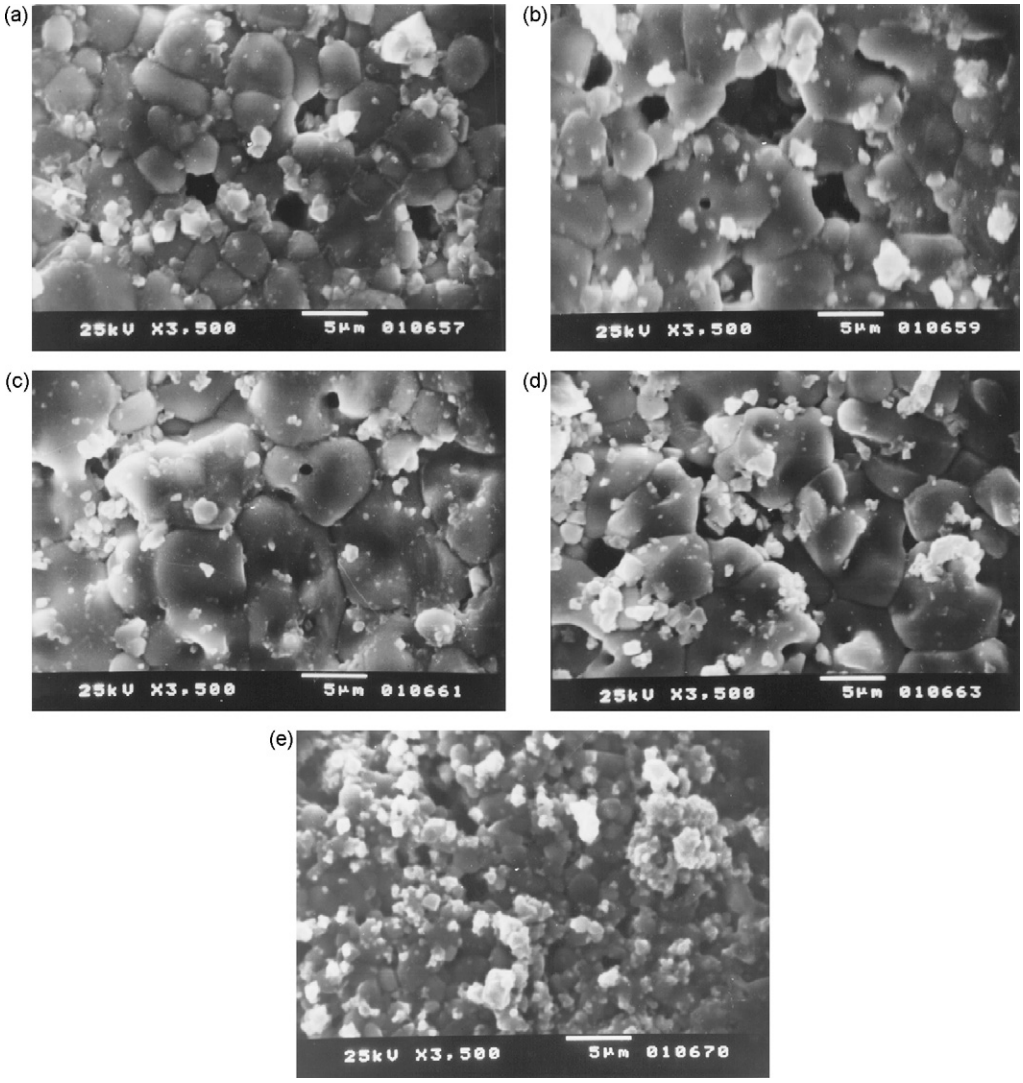

Fig. 1. Surface microstructures of specimens containing Sb_2O_3 for various Li_2CO_3 concentrations: (a) 0 ppm, (b) 20 ppm, (c) 50 ppm, and (d) 100 ppm (CW specimens).

mittivity and N_d: total charge density in the depleted region, assumed to be the donor density of majority charge carriers.

Amphoteric lithium might act as a donor or an acceptor (h) whether it is in interstitial or substitution location:

$$Li_2O + ZnO \rightarrow 2\,Li_i^{\circ} + 2\,e + ZnO \quad (4)$$

$$Li_2O + ZnO \rightarrow 2\,Li_{Zn}' + 2\,h + ZnO \quad (5)$$

A self-compensation might arise leading to:

$$Li_2O + ZnO \rightarrow Li_i^{\circ} + Li'_{Zn} + ZnO \quad (6)$$

Only Eq. (4) or (6) might explain an increase in the lattice parameters [19] (very recent work suggests also the possible formation of the complex: Li_{Zn}–H–Li_{Zn} leading to an extra acceptor state observed in spectroscopy [19]).

Equation (4) and (5) have been recently revised in order to let the cation vacancy concentration dependent on the amount of Li occupying the interstitial and substitutional sites [20]:

$$Li_2O + 2\,V_{Zn} \rightarrow 2\,Li_{Zn}' + O_O + 2h \rightarrow 2Li_i + V_{Zn} + \acute{e} + O_O \quad (7)$$

The decrease of the conductivity of single crystal or thin films [19–21] is explained by migration of lithium interstitial in substitution:

$$Li^{\circ}_i + \acute{e} \rightarrow Li_{Zn}' + Zn^{\circ}_i \quad (8)$$

or less likely

$$Li^{\circ}_i + \acute{e} \rightarrow Li_{Zn}' + V^{\circ}_O \quad (9)$$

Eqs. (8) and (9) lead to a reduction in donor density N_d although (4) and (7) improve N_d. Our electrical measurements show an increase of the non linear coefficients which are related to α. From where, one can deduce that the majority of the lithium atoms which penetrate into the ZnO network occupy a substitution position. They react like acceptors and collect free

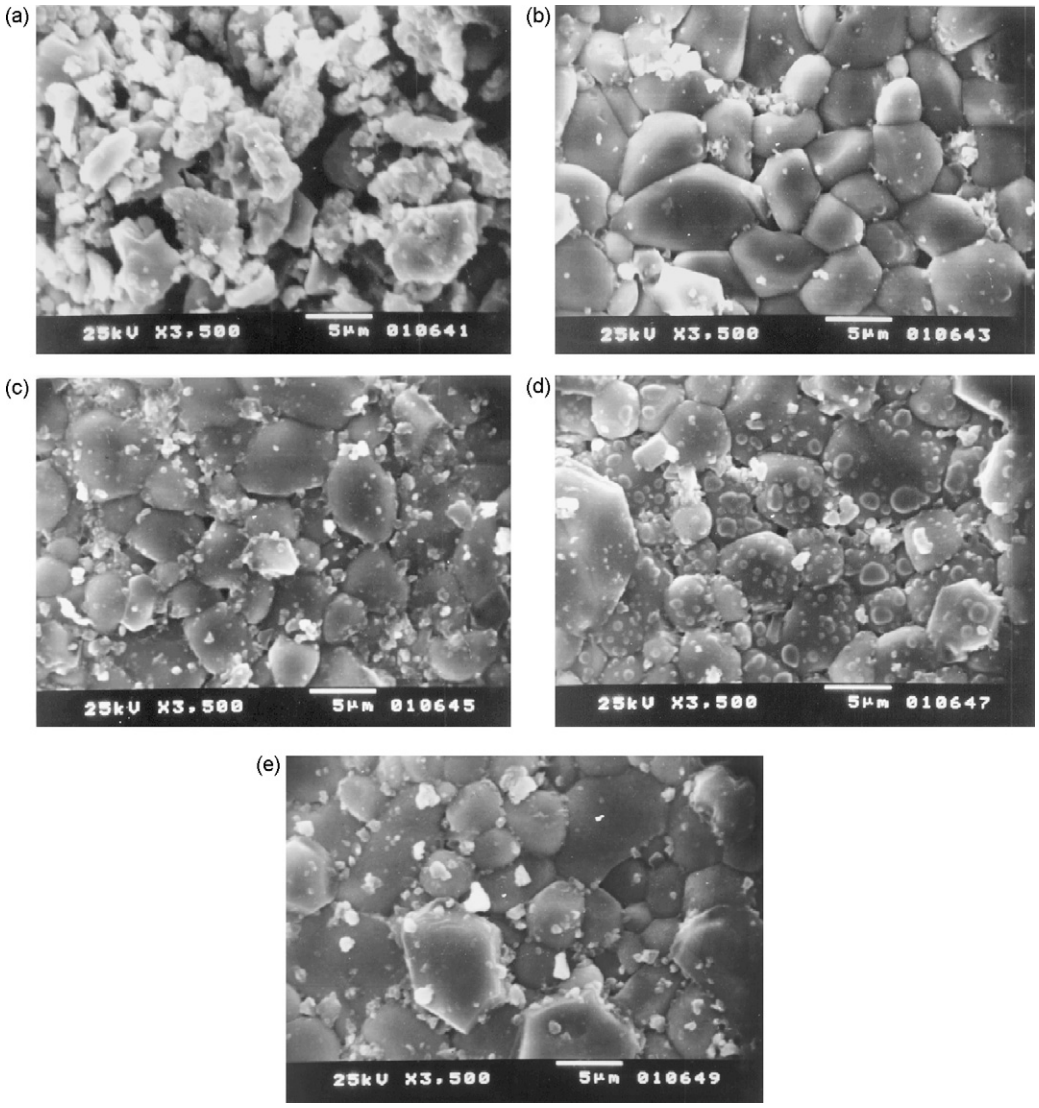

Fig. 2. Surface microstructures of the specimens without Sb_2O_3, with various concentrations of Li_2CO_3: (a) without Li_2CO_3, (b) 20 ppm, (c) 50 ppm, (d) 100 ppm, and (e) 200 ppm (CO specimens).

electrons in the network [22]. Therefore, the donor density N_d strongly decreases while making increase the barrier of potential. This assumption is acceptable, because in all the studied cases, Li_2CO_3 which one adds to the initial composition reduced the varistor energy absorption capability (Table 2). This decline would find its origin in N_d reduction which diminishes the varistor conductivity and causes a faster saturation for relative low density of currents.

The packing of surface state density N_s is related to Q_i and might therefore be the cause of the barrier of potential height increase at the grain boundaries. One can advance here the assumption whereby when the Li_2CO_3 content in the initial chemical composition increases, part of the lithium atoms does not penetrate any more in the ZnO grains, they remain within the grain boundaries. This assumption is realistic since high resolution secondary ion images carried out on Li_2CO_3-doped ZnO reveal that in samples doped with 0.05% Li_2CO_3, Li is mainly located in grain boundaries [20]. They form defects; the surface state density N_s might increase, boosting the barrier of potential at grain boundaries.

In conclusion, in the composition with Sb_2O_3 the lithium has a double effect. On the ZnO grain size it can support the spinels formation which blocks the grain growth. On the barrier of potential, it makes decrease N_d and simultaneously increases N_s and consequently it raises the barrier of potential to the grain boundaries.

3.2. Composition without Sb_2O_3

Formulations without Sb_2O_3 were prepared in order to check the lithium ions influence separately to that of antimony. The following observations are formulated:

3.2.1. Without Li_2CO_3

Two remarkable changes appear compared to the composition which contains antimony oxide. First, E_s is relatively low as it might be expected from Eq. (1) (Table 2 and Fig. 2). The absence of antimony results in the nonexistent Zn–Sb phases precipitated in the grain boundaries. This lead to about 40% larger ZnO grains: 12 to 19 μm. Second, (A) reaches rather high values (>100 J/cm^3). In this case, the conduction section between two grains is not anymore narrowed by intergranular phases of spinels. It reaches the greatest possible value, and ensures passage of the highest possible density of current.

3.2.2. Li_2CO_3 = 20, 50 and 100 ppm

E_s increases from 257 V/mm (20 ppm of Li_2CO_3) to 315 V/mm (100 ppm of Li_2CO_3). In these cases, ZnO grains the size of the grains decreases from 19 to 12 μm (Table 2). That thus involves a significant increase in the threshold field (Table 2).

The increase of the non linearity is interpreted as the result of a decrease of the donor density. In addition, in these cases, (A) is maintained at relative high values of approximately 100 J/cm^3. The conduction section is not narrowed by phases precipitated in the grain boundaries at one can expect when antimony is added. The largest value 115 J/cm^3 obtained when the Li_2CO_3 content is optimum, i.e. 100 ppm. After having reached this value, (A) slashes drastically. This might be interpreted by a consecutive decrease of the grains conductivity.

4. Conclusion

With the benefit of Sb_2O_3, a very significant influence of lithium on the electric properties of doped-ZnO varistor has been founded. Very small quantities of lithium added to ceramic formulations causes a significant increase in both the threshold field and the non linearity. This comes owing to the fact that first lithium acts as a grain growth inhibitor, second it makes decrease the donor density N_d and thus increase the barrier of potential. Ceramic compositions without antimony have maintained a high value of energy absorption capability. This behavior is interpreted by the lack of secondary intergranular $Zn_7Sb_2O_{12}$ phases at the grain boundaries leading to higher density of current by improving the effective current path from one ZnO grain to another.

References

[1] M. Matsuoka, Jpn. J. Appl. Phys. 10 (6) (1971) 736.
[2] K. Eda, I.E.E.E. Electr. Insul. Mag. 5 (6) (1989) 28.
[3] E. Olsson, L.K.L. Falk, G.L. Dunlop, R. Osterlund, J. Mater. Sci. 20 (1985) 4091.
[4] T.K. Gupta, J. Am. Ceram. Soc. 73 (7) (1990) 1817.
[5] L.M. Levinson, H.R. Philipp, Ceram. Bull. 65 (4) (1986) 639.
[6] M. Inada, Jpn. J. Appl. Phys. 17 (3) (1978) 106.
[7] M. Inada, Jpn. J. Appl. Phys. 19 (3) (1980) 419.
[8] M.T. Takemura, M. Kobayashi, Y. Takada, K. Sato, J. Am. Ceram. Soc. 70 (4) (1987) 237.
[9] M. Inada, Jpn. J. Appl. Phys. 18 (8) (1979) 1439.
[10] A. Bui, H.T. Nguyên, A. Loubière, J. Phys. D: Appl. Phys. 28 (1995) 7743.
[11] K. Jinho, T. Kimura, T. Yamagushi, J. Am. Ceram. Soc. 72 (8) (1989) 1390.
[12] J. Wong, J. Appl. Phys. 46 (4) (1978) 2407.
[13] J. Kim, T. Kimura, T. Yamaguchi, J. Mater. Sci. 24 (7) (1989) 2581.
[14] D. Clarke, J. Am. Ceram. Soc. 82 (3) (1999) 485.
[15] B.K. Meyer, J. Stehr, A. Hofstaetter, N. Volbers, A. Zeuner, J.I. Sann, Appl. Phys. A: Mater. Sci. Process. 88 (1) (2007) 119–123.
[16] K. Mukae, K. Tsuda, I. Nagasawa, J. Appl. Phys. 50 (6) (1979) 4475.
[17] A. Rohatgi, S.K. Pang, T.K. Gupta, W.D. Stranb, J. Appl. Phys. 63 (11) (1988) 5375.
[18] F. Greuter, G. Blatter, Electrical properties of grain boundaries in polycrystalline compound semiconductors, Semicond. Sci. Technol. 5 (1990) 111–137.
[19] O. Yavuz, B. Banu, A. Hasan, Appl. Sur. Sci. 253 (10) (2007) 4593–4598.
[20] N. Tsubasa, S. Isao, M. Katsuyuki, Y. Takahisa, H. Hajime, I. Yuichi, Nuclear Instruments and Methods in Physics Research, Sect. B: Beam Interact. Mater. Atoms 232 (2005) 343–347.
[21] S. Fujihara, C. Sasaki, T. Kimura, Effects of Li and Mg dopin on microstructure and properties of sol–gel ZnO thin films, J. Eur. Ceram. Soc. 21 (2001) 2109–2112.
[22] T. Miyoshi, K. Maeda, K. Takahashi, T. Yamazaki, Grain Boundary Phenomena in Electronic Ceramics. (L.M. Levinson, D. Hill. Am. Ceram. Soc., Columbus, OH, 1981).